A SYSTEMATIC VIEW OF OPTICAL ABSORPTION
SPECTRA IN THE ACTINIDE SERIES*

W. T. Carnall

Chemistry Division, Argonne National Laboratory
Argonne, Illinois, USA

DISCLAIMER

A SYSTEMATIC VIEW OF OPTICAL ABSORPTION
SPECTRA IN THE ACTINIDE SERIES*

W. T. Carnall

Chemistry Division, Argonne National Laboratory
Argonne, Illinois, USA

In recent years sufficient new spectra of actinides in their numerous valence states have been measured to encourage a broader scale analysis effort than was attempted in the past. Theoretical modelling in terms of effective operators has also undergone development. Well established electronic structure parameters for the trivalent actinides are being used as a basis for estimating parameters in other valence states and relationships to atomic spectra are being extended. Recent contributions to our understanding of the spectra of 4+ actinides have been particularly revealing and supportive of a developing general effort to progress beyond a preoccupation with modelling structure to consideration of the much broader area of structure-bonding relationships. We summarize here both the developments in modelling electronic structure and the interpretation of apparent trends in bonding.

Introduction

In summarizing recent contributions to the optical spectroscopy of the actinides, the discussion will focus on the spectra observed or in some cases predicted for each valence state, but in the context of a developing systematic interpretation. Our ability to model f-element spectra has shown marked and progressive improvement with time, but as with experiment, many challenges remain for the future.

If we restrict consideration to elements and states where characteristic f→f transitions in actinide spectra have been measured, we see from Figure 1 that there are two long series and three abbreviated ones on which to focus attention. Theory will be of particular advantage in the abbreviated series where it can help organize observations and predict the energies of unobserved transitions.

The objective is to progress from observation of spectroscopic features to their interpretation in terms of a predictive theoretical model which views these features as arising from transitions within a system of energy levels. While prediction of missing transition energies, or indeed of the complete structure in unexplored systems, is of importance, a useful model will at the same time provide a link to understanding other types of experimental results such as magnetic interactions. The ability to model structure has led further to the ability to model the intensities of certain f-electron spectra in absorption. Such intensity modelling leads to computation of radiative relaxation behavior and in turn forms the basis for predicting possible lasing transitions.

Trivalent Actinide Ion Spectra

There are several reasons for beginning with a brief discussion of trivalent actinide spectra. First, it is the most completely characterized series both from the experimental and theoretical points of view (1-3). Our theoretical interpretation of the observed crystal-field structure (in D_{3h} symmetry) is complete in the sense that there is excellent correlation between computed and experimentally observed transition energies, and it does not appear to be profitable to further expand the current effective operator model of electrostatic and spin-orbit interactions. This model is summarized in Figure 2. It is used to describe f-electron structure in all valence states. Since summaries of the model interactions and experimental details are available (2,4), we limit discussion here to some newer developments.

One of the important generalizations that has become evident in recent years is the relationship between the electrostatic and spin-orbit parameters determined from spectra of ions doped into host crystals, and the parameters characteristic of certain configurations in atomic spectra. Correlation between An^{3+} parameters and those for the $5f^N 7s^2$ configurations in second

spectra (An II) have been discussed previously (5), but further experimental as well as interpretive progress has been made.

The An^{3+} spectra in crystal hosts are well suited to such correlations since the crystal-field effects are small relative to the electrostatic and spin-orbit interactions. Thus the center of gravity of the crystal-field components of a level becomes the analog of the gaseous free-ion level. Although there are still very few actinide free-ion analyses available, the number of cases where correlations can be made is growing. A recent summary of parameter values for low Pu configurations (6) illustrates the close relationship between the structure of the $5f^57s^2$ configuration in Pu II and that for $5f^5$ in $Pu^{3+}:LaCl_3$, Table 1. Thus the 5f-core electrons are not much influenced by either the shielding of the $7s^2$-shell in An II or the perturbation introduced by the ligands that form the primary coordination sphere in An^{3+}. For Pu II, the parameters of the f^5ds-configuration are also found to be nearly the same as those for f^5s^2.

The importance of the connection between free-ion and crystal spectra lies in its synergistic effect to both areas of analysis. For example, there are many analyzed spectra for An^{3+} in crystal hosts, and thus the parameters from that source form a secure basis for estimating parameters for appropriate atomic spectra. However, as we examine An^{2+} spectra, the data base is sparse; indeed spectra of light actinides like Pu^{2+} have not yet been reported. However, as will be shown subsequently, parameters for lighter actinides can be extrapolated from approximate analyses of Cf^{2+} and Es^{2+}. Some independent method of verifying both the estimates and the extrapolated parameters is clearly essential. Here we point out that energy level parameters determined for $CfCl_2$ do indeed correlate well with a recent parametrization of experimental results for Cf I, Table 1 (2,7). The extrapolated spin-orbit parameter for Cm^{2+} is also in agreement with that for Cm I (2). Further, in Pu I f^6s^2, we see good correlation with F^2, F^4, and ζ for extrapolated values for Pu^{2+}, but F^6 is too large. This may simply be the result of a gradual departure of observed from extrapolated values over a whole series. The fit parameters for Pu I f^6ds do not correlate well with those of f^5s^2; however, the two configurations are widely separated in energy whereas the counterparts in Pu II have nearly the same energy relative to Pu II f^6s (6).

One of the uses of the state eigenvectors derived from effective operator parameters is in the computation of the matrix elements required in the Judd-Ofelt transition intensity theory (8,9). Use of this theory has made possible an excellent correlation between computed and observed band intensities in trivalent lanthanide crystal and solution spectra as well as in the solution spectra for the heavier members of the trivalent actinide series (4). Until recently it was difficult to uniquely define intensity parameters consistent with the light half of the actinide series, Figure 3, where the energy level structure is condensed and state characterization more difficult. We consider here an important concept that has emerged from the detailed interpretation of band intensities via the theory (1).

If we compare intensities of $f \to f$ transitions at $< 25000 \text{ cm}^{-1}$ in the light and heavy actinides, we see by inspection a striking change over the series with the very intense bands in U^{3+}(aquo) contrasted to much weaker bands in Bk^{3+}, Cf^{3+}, and Es^{3+}.

A modification of the relationship derived by Judd can be written:

$$P_{ED} = \frac{8\pi^2 mc}{3h} \cdot \frac{\sigma}{(2J+1)} \chi \sum_{\lambda=2,4,6} \Omega_\lambda (\psi J||U^{(\lambda)}||\psi'J')^2$$

and accounts for the electric dipole oscillator strength, P_{ED}, of observed transitions summed over the crystal-field components of each excited state with center at $\sigma \text{ cm}^{-1}$. J refers to the ground state and χ is the refractive index correction term. The sum is over three parameters Ω_λ, which are coefficients of the unit tensor operators $U^{(\lambda)}$. It was recently shown that for An^{3+}(aquo), Ω_2 does not make a significant contribution to the observed intensity so that in fact the value of P_{ED} can be computed in good agreement with the intensity of each transition in the spectrum via two fit parameters Ω_4 and Ω_6 for each An^{3+}(aquo) (1). It has been found that the values of the parameters, not the matrix elements of $U^{(\lambda)}$ mirror the overall change in intensity. Thus, the important insights in this case derive by examining the interactions which are included in the parameters, Ω_λ.

The details of the first principles calculation of Ω_4 and Ω_6 for each of the An^{3+}(aquo) ions have been given recently (4); we summarize here. The part of the interaction that is dependent on radial moment integrals of the form

$$R(t) = (n\ell|r|n'\ell')(n\ell|r^t|n'\ell')$$

which couple the $5f^N$-configuration (nℓ) to perturbing configurations of opposite parity, (n'ℓ'), shows the same rapid decrease in magnitude exhibited by the change in intensity as a function of atomic number, Z (1). The values of R(t) for Am^{3+} and Cm^{3+} suggest a transition region to the much smaller intensities (and moment integrals) characteristic of Bk^{3+}(aquo) and the trans Bk ions. A similar treatment of the lanthanide aquo ions reveals anomalously intense bands in Pr^{3+}(aquo) and Nd^{3+}(aquo) which suggest that these ions may occupy a position in the lanthanide series comparable to that of Am^{3+}(aquo) and Cm^{3+}(aquo) in the actinide series. The abrupt change in intensity is therefore correlated with the magnitude of the coupling of the f^N and opposite parity configurations in both the actinide and lanthanide series.

Trends in experimental properties such as magnetism in the actinide and lanthanide metals parallel the intensity change in An^{3+}; however the further relationship between magnetism and bonding has been established using band structure calculations (10).

Magnetic moments arise when orbitals are localized, that is, when there is little bonding. With increasing atomic number for the lanthanide and actinide metals and alloys, nuclear charge increases the localization of inner shell d- and f-orbitals. A change from delocalized (bonding) to localized moment (non-bonding) behavior is indicated early in both the 4f- and 5f-series as shown in Figure 4, which is an abbreviated version of a figure given by Smith and Kmetko (11). The crossover from delocalized to localized behavior in the 3d series is included in the figure to emphasize the intermediate behavior of the actinide series, i.e. occupying a position between the 4f- and 3d-series when this type of comparison is made (10). Particular interest is focussed on the crossover region because it is there that for some metals and alloys the balance can be shifted by such parameters as pressure, temperature or dilution.

We have correlated the decrease in intensity of the An^{3+}(aquo) and Ln^{3+}(aquo) transitions with a decrease in the magnitude of a radial moment integral term, R(t). Since these integrals were computed using free-ion wave functions, they are in fact simply reflecting the well-known sudden contraction of the 4f- and 5f-orbitals in the early members of each series (12). The situation is therefore the counterpart of that described in the band structure calculations for the metals (10). The decrease in transition

intensity in the trivalent ions does therefore track an increasing locali-
zation of the 4f- and 5f-electrons.

As Brewer (13) has pointed out, abnormal behavior in the actinides and
lanthanides may suggest either a change in f-electron localization or a pro-
motion of f-electrons to d- or other orbitals that allows them to participate
in bonding. It is the latter that is suggested here by the moment integral
correlation.

Systematic Calculation of Energy Level Structure

While spectra of compounds and solutions containing actinides in other
than the tripositive valence state are well known, systematic analyses of
their electronic structures are very much in the developmental stage. The
trend in the experimentally determined F^k and ζ parameters for the 3+
actinides as a function of Z very closely matches that in the corresponding
Hartree-Fock values, Figure 5. The energy differences, $E_{HF}-E_{EXPT} = \Delta P$, are
found to be nearly constant over the series. Values of the two-body and
three-body effective operators are also essentially constant as a function of
Z, and indeed the magnitudes of these latter parameters for the actinides are
very nearly those deduced for the lanthanides (2,4,14).

The Hartree-Fock values for the Slater and spin-orbit integrals relevant
to each valence state have been computed (2,15). Based on the consistency of
the ΔP values for trivalent actinides and lanthanides, an initial analysis
assuming similar behavior in other valence states has been proposed (16). The
advantage of this method is that only a single case in which the energy level
parameters have been determined from experimental data is needed to establish
a characteristic value of ΔP, and thus to determine parameters for each member
of a series.

Divalent Actinide Ion Spectra

Efforts to prepare divalent actinide compounds and analyze their spectra
have so far been less successful than was the case for the lanthanides, for
which the divalent ion for each member of the series could be stabilized in
CaF_2 (17). Since the available spectroscopic results for divalent actinides
are fragmentary (18-21), the extrapolation procedure outlined above is
applicable. An attempt has now been made to account for the observed spectral

features shown in Figure 6, and then to predict the energies of characteristic bands not yet reported but possibly accessible to observation (6,16). Since a full description of the analysis has not been published (22), some of the conclusions are outlined below.

Crystal-field splitting for the divalent actinide halides appears to be no larger than that for the trivalent case; the structure model was consequently limited to free-ion considerations. The model energy level schemes for An^{2+} based on data for Cf^{2+} and Es^{2+} are plotted in Figure 7 where the lowest levels in the $5f^{N-1}s$ and $5f^{N-1}d$ configurations are also indicated (23). Additional absorption features not previously reported are predicted in the near infrared range in both Cf^{2+} and Es^{2+} (16). The value of the "predictions" for f→f transitions in all cases depends strongly on the extent of the optical windows to be expected, i.e. the energy at which the absorption due to f→d transitions will first be observed.

The energies quoted by Brewer (23) are for the gaseous free-ion. An estimate of the extent to which the actinide free-ion energy would be lowered by ligand-field interaction was based on the corresponding results for $Ln^{2+}:CaF_2$, where the energy difference was ~ 8000 cm^{-1} (17). There are several members of the Ln^{2+} series in which the ground state is not in the $4f^N$-configuration, and this is also indicated to be the case for some An^{2+}.

While $5f^{N-1}6d$ states lie lowest over $5f^N$ for the light half of the series, this changes at Cm^{2+}. In the heavier members the ground state of the $5f^{N-1}6s$ configuration is predicted to be lower in energy than that of $5f^{N-1}d$ (23). In $Ce^{3+}:CaF_2$, the $f^N \rightarrow f^{N-1}s$ transitions were a factor of 100 weaker than those corresponding to $f^N \rightarrow f^{N-1}d$ (24). A similar relationship is assumed as a first approximation in the analogous 5f-case. The occurrence of f→d transitions in Es^{2+} and Cf^{2+} approximately 8000 cm^{-1} lower in energy than that predicted for the lowest free-ion f→d transition would result in expectation of rising absorption near 19000 cm^{-1} and 16000 cm^{-1}, respectively. In both cases broad, increasingly intense absorption features do appear near these energies. In the case of Am^{2+}, the intense broad bands earlier attributed to possible f→d transitions are reported in the predicted range (18).

In Bk^{2+} and Pu^{2+}, as in Am^{2+}, it may be possible to observe the first excited state in the f^N-configuration before f→d absorption becomes

predominant, but in each case the only f→f transitions observable in absorption are expected to lie well into the infrared range. In Np^{2+} and Cm^{2+}, the ground configuration will probably be $f^{N-1}d$ instead of f^N because of the stabilization energy. The $5f^36d$-configuration lies lowest in U III; Th^{2+}, Pa^{2+} and U^{2+} all have non-f^N ground configurations (23). Because of the predicted large energy gap between the ground ($^3S_{7/2}$) and first excited ($^6P_{7/2}$) states in Am^{2+}, fluorescence near 14000 cm^{-1} is predicted to occur.

Quadrivalent Actinide Ion Spectra

Several recent contributions have considerably expanded our understanding of the spectra of the quadrivalent actinides. The identification of the free-ion energy levels in the U V $5f^2$-configuration is now complete (25,26), and this provides a valuable basis of comparison for the analyses of spectra in condensed phases. The number of reliable detailed analyses of spectra in crystals is very small, and, with important exceptions, involves primarily the Pa^{4+} and U^{4+} ions, i.e. $5f^1$ and $5f^2$. An experimental deficiency is the apparent lack of a suitable host lattice into which a broad range of An^{4+} ions can be doped. The excellent results with $ThCl_4$ and $ThBr_4$ as hosts may end at Np^{4+} where both the 4+ and 3+ oxidation states have been observed (27).

The published analysis of U^{4+}:$ThBr_4$ based on the identification of spectroscopic features identified with both D_{2d} and limiting D_2 sites (28,29), and the similar crystal-field parameters deduced for Pa^{4+}:$ThCl_4$ (30) have provided an extremely important new dimension to the interpretation of An^{4+} spectra. A reinterpretation of the spectrum of UCl_4 (31) has also led to energy level parameters that are quite similar to those for U^{4+}:$ThBr_4$.

Somewhat in contrast to observations made with trivalent ions, there appear to be two extremes of crystal-field splitting into which many of the known spectra of U^{4+} can be divided. A good example of the high-symmetry (O_h), large-field case is that of U^{4+} in Cs_2UCl_6 (32) where the analysis was recently augmented by an extensive interpretation of intensities in the observed vibronic transitions (33). In spectra of this type the zero phonon transitions are not observed directly, but are located by vibrational patterns built on the missing electronic centers.

The lower symmetry (typically D_{2d}), weaker field case is now illustrated by the U^{4+}:$ThBr_4$ spectrum (28). If we use Auzel's scalar crystal-field

strength parameter, N_v (34), as a basis for comparison, we find $N_v = 5732$ cm^{-1} for U^{4+}:ThBr$_4$ and a factor of two greater, $N_v = 11922$ cm^{-1} for U^{4+}:Cs$_2$UCl$_6$. For quadrivant spectra this difference has pronounced consequences. The crystal-field splitting in U^{4+}:ThBr$_4$ is much larger than for example in U^{3+}:LaCl$_3$ (35), but groups of levels can still be recognized as possessing a principal SLJ-character. This is indicated in Figure 8. In the high symmetry cases, strong J-mixing is the rule rather than the exception and treatment of the spectroscopic data that relies on predominant SLJ-character in a group of levels would generally be a poor approximation. The energy level structure in U^{4+}:ThBr$_4$ provides a relatively good correlation with the observed spectrum of U^{4+}(aquo) as indicated by centers of gravity of absorption bands included in Figure 8, and an intensity analysis of U^{4+}(aquo) has been reported (36). Conversely, a successful analysis of this type would not have been expected based on the eigenvectors for U^{4+}:Cs$_2$UCl$_6$.

From a comparison of the spectra of iso-f-electronic U^{3+}(aquo) and Np^{4+}(aquo), one can recognize a similarity in grouping of absorption features as well as relative intensities, and this extends further to the Np^{3+}–Pu^{4+}(aquo) ion couple (16,37). Thus, based on the U^{4+}:ThBr$_4$ results it is now possible to develop a systematic energy level analysis for An^{4+} which can be compared to available data for An^{4+}(aquo), as well as to spectra of An^{4+} in concentrated fluoride salt solutions and to the spectrum of BkF$_4$ (38).

The crystal-field strengths of the borodeuterides of both U^{4+} and Np^{4+} were recently shown to be even greater than that associated with U^{4+}:Cs$_2$UCl$_6$. Absorption bands attributed to zero-phonon transitions were identified in the borodeuterides (T$_d$-symmetry) although the observed structure was primarily vibronic in character (39,40). A crystal-field strength parameter $N_v = 15406$ cm^{-1} for U(BD$_4$)$_4$:Hf(BD$_4$)$_4$ compared to 11922 cm^{-1} for U^4:Cs$_2$UCl$_6$ suggests even greater J-mixing, and indeed 70% of the states have a single SLJ-character of $< 65\%$. Several assignments that await confirmation, for example by independent intensity calculations, appear to be critical to the interpretation. If these assignments were to be proven incorrect, the authors suggest that this would represent a case in which there is a fundamental inconsistency with the one particle model of the crystal-field.

Penta- and Higher-valent Actinide Ion Spectra

Actinide ions with well defined, stable, and readily accessible valence states greater than (IV) are confined to the light half of the 5f-series. While a large number of stable compounds are known, and spectra have been recorded in solutions and in the gas phase as well as in solids, there have been few attempts to develop detailed energy level analyses except in the least complex cases. The increased multiplet splittings with increased charge state for f^1-configurations in essentially O_h-symmetry are indicated in Figure 9, (22). Both spin-orbit and crystal-field parameters are increasing significantly for the ions shown, but there appears to be a particularly large increase in the crystal-field parameters for NpF_6 compared to those for $LiUF_6$.

Pentavalent Actinide Ion Spectra

Although there are a number of published attempts to analyze An(V) spectra dating from the early 1960's, compound purity has been a factor that has limited the value of some of the interpretation. Of the existing analyses, except for $CsNpF_6$, all involve U(V). Much interest has centered on $CsUF_6$ and its structural analogs because the spectra of isostructural Np(V) and Pu(V) compounds have been reported (41,42). A new complete analysis of the spectrum of $CsUF_6$ was recently presented (43). The spectroscopic features characteristic of $CsUF_6$ are common to a large group of complex salts containing U(V) (44), including as well UCl_5 (45).

There have been two recent analyses of U(V)-containing compounds in which the spectra are quite different from that observed in $CsUF_6$. Both α-UF_5 and β-UF_5 spectra were analyzed assuming a crystal-field dominated by weak covalent rather than electrostatic interactions (46). The same approach was embodied in elucidating the spectrum of $RbUF_6$ (47). Spectroscopic features attributed to UF_5 molecules generated by laser photolysis of UF_6 have also been identified in the 350-700 nm range (48).

The spectrum of $CsNpF_6$ as originally analyzed was reinterpreted by Poon and Newman (49), but work in progress (50) has failed to confirm important features of the spectrum as originally published, so further experimental and interpretative studies are indicated. Recent experimental studies of isostructural $CsUF_6$, α-$NaUF_6$, and $LiUF_6$ revealed a rich vibronic spectrum

associated with what were interpreted as magnetic-dipole transitions in D_{3d} (nearly octahedral) symmetry (43).

If we use ligand-field and spin-orbit parameters established for $CsUF_6$ as the basis of a predictive model, and couple this with electrostatic parmeters of the same order as suggested for $CsNpF_6$ (49), then the resulting energy level schemes for $CsNpF_6$ and $CsPuF_6$ obtained by extrapolation appear to be consistent with available data (6).

Hexavalent Spectra

The actinide hexafluorides form a unique group of volatile molecular species with a long established relationship to the technology of isotope separation. While UF_6 has no f-electrons in open shells, f→f transitions in both NpF_6 and PuF_6 are well known. The detection of fluorescence in the selective excitation of NpF_6 and PuF_6, at energies consistent with the first excited states found in absorption, was recently reported (51). Much of the current spectroscopic interest in PuF_6 is associated with its photochemical reactions, but in the course of this effort electronic structure was also revealed; fluorescing states at 1.0 μ have been reported and fluorescence at 2.3 μ confirmed (52). Estimates of the energy level structures in PuF_6 and AmF_6 have been made (6).

Neither UF_6 nor uranyl (UO_2^{2+})-compounds exhibit the f→f transitions usually considered characteristic of the actinides, so measurement and interpretation of U(VI)-spectra constitutes a unique area of actinide spectroscopy which continues to receive considerable attention. The observed transitions are interpreted as involving the excitation of a bonding electron into non-bonding f-orbitals of the U(VI), and they exhibit a clear symmetry dependence. In one of a series of communications on actinyl-ions, Denning and coworkers recently reported the measurement and interpretation of spectra of $Cs_2UO_2Cl_4$ doped with Br^- (53). Doping removed the center of symmetry with respect to the U(VI) and thus permitted observation of electric-dipole transitions in a crystalline compound previously explored in the pure state (54,55). The results supported the original interpretation (55) of the transitions as involving the $\sigma_u \delta_u$ and $\sigma_u \phi_u$ configurations of UO_2^{2+} in contrast

to an alternate description that had been proposed (56). However, reassign-
ment of certain excited states was made consistent with recent ab initio
calculations (57).

Several f→f transitions as well as charge-transfer type transitions were
identified in a spectroscopic study of Np(VI) doped into both $Cs_2UO_2Cl_4$ and
$CsUO_2(NO_3)_3$ (58,59). The spin-orbit and ligand field parameters for the $5f^1$-
configuration were computed using a perturbation method. Gorshkov and
Mashirov have also assigned electronic transition energies in $Cs_2NpO_2Cl_4$ (60)
but only partially in agreement with Denning and coworkers. No interpretation
has been made of reported spectra for An(VII) and thus, it is not clear
whether f→f transitions have been observed.

Closing Speculations

Aside from the trivalent and divalent series, much of the recent inter-
pretive and experimental effort is seen to have been centered on uranium, in
part as a possible first member of an isostructural series. Progress has
been made in analyzing such spectra but there are also instances of disconti-
nuity between the interpretation of spectra in structurally similar compounds
of U and Np. It is useful to remember that $U^{3+}:LaCl_3$ was the last member of
that family to yield to analysis, and it also exhibits the poorest correlation
between theory and experiment of any member of the series $An^{3+}:LaCl_3$ or
$AnCl_3$. The vibronic structure so characteristic of Cs_2UCl_6 was not reported
in isostructural Cs_2NpCl_6. It may be well to retain some skepticism as to how
representative the behavior of uranium can be expected to be. It frequently
affords the simplest f-electronic configuration for analysis; the correspond-
ing Np compounds may turn out to be more representative of the series.

Table 1.

f^N Parameter Values for Low Pu and Cf Configurations (in cm^{-1})[a]

	Pu II[b] (f^5s^2)	Pu³⁺:LaCl₃[b] (f^5)	Pu II[b] (f^5ds)
F^2	49066 (770)	48670 (154)	4923C (1243)
F^4	39640 (719)	39188 (294)	37215 (1468)
F^6	26946 (785)	27493 (153)	[27918]
α	[32.55]	29.7 (0.4)	[32.55]
β	[-652]	-671 (15)	[-652]
γ	[1200]	1067 (79)	[1200]
ζ	2275 (27)	2241 (2)	2263 (11)

	Cf I[c] ($f^{10}s^2$)	CfCl₂[d] (f^{10})
F^2	56503 (169)	56711
F^4	41584 (745)	41172
F^6	35565 (299)	35274
α	[30]	[30]
β	-808 (62)	[-800]
γ	1441 (152)	[1200]
ζ	3388 (6)	3446

	Pu I[b] (f^6s^2)	PuCl₂[d] (f^6)	Pu I[b] (f^6ds)
F^2	45144 (624)	43930	[49300]
F^4	31656 (1174)	32570	[39500]
F^6	[24452]	28850	[27460]
α	[32.55]	[30]	[35]
β	[-652]	[-800]	[-900]
γ	[1200]	[1200]	[1100]
ζ	2063 (20)	2118	2233

[a]Values in parentheses are the mean errors in the computed parameters. Brackets indicate the value was not varied in the least squares fitting process.
[b]Additional parameters are given or cited in Reference 6.
[c]These and further parameters are discussed in Reference 2.
[d]Estimated from experimental results or extrapolated.

References

1. W. T. Carnall, H. Crosswhite, and K. Rajnak, Proc. Int. Symp. on Rare Earths spectroscopy, Wroclaw, Poland, 1984, in press.

2. H. M. Crosswhite and H. Crosswhite, J. Opt. Soc. Am., B1, 246 (1984).

3. Y. M. Poon and D. J. Newman, J. Phys. B. At. Mol. Phys., 16, 2093 (1983).

4. W. T. Carnall, J. V. Beitz, H. Crosswhite, K. Rajnak, and J. B. Mann, "Systematics and the Properties of the Lanthanides," NATO ASI Series, S. P. Sinha, ed., D. Reidel Publishing Company, Boston, 1983, pp. 389.

5. J. Blaise, J.-F. Wyart, J. G. Conway, and E. F. Worden, Physica Scripta, 22, 224 (1980).

6. J. Blaise, M. S. Fred, W. T. Carnall, H. M. Crosswhite, and H. Crosswhite, ACS Sympos. Series, 216, 173 (1983).

7. J. Blaise, J. G. Conway, and E. Worden, personal communication quoted in Reference 2.

8. B. R. Judd, Phys. Rev., 127, 750 (1962).

9. C. S. Ofelt, J. Chem. Phys., 37, 511 (1962).

10. H. H. Hill, "Pu 1970 and Other Actinides," W. N. Miner, ed., Am. Inst. Mechanical Engineers, New York, 1970, pp. 2.

11. J. L. Smith and E. A. Kmetko, J. Less-Common Metals, 90, 83 (1983).

12. B. G. Wybourne, "Spectroscopic Properties of the Rare Earths," Interscience Publishers, New York, 1965.

13. L. Brewer, "Systematics and the Properties of the Lanthanides," NATO ASI Series, S. P. Sinha, ed., D. Reidel Publishing Company, Boston, 1983, pp. 17.

14. H. M. Crosswhite, Colloques Internationaux du C.N.R.S., Spectroscopie de Elements de Transition et des Elements Lourds dans les Solides, 28 Juin-3 Juillet 1976, Editions due C.N.R.S., Paris, 1977, pp. 65.

15. J. P. Desclaux and A. J. Freeman, "Handbook on the Physics and Chemistry of the Actinides," ed., A. J. Freeman and G. H. Lander, Elsevier Science Publishing Co., New York, 1984, Vol. 1, pp. 1.

16. W. T. Carnall and H. M. Crosswhite, "The Chemistry of the Actinide Elements," eds., J. J. Katz, G. T. Seaborg, and L. R. Morss, Chapman and Hall Ltd., London, in press.

17. D. S. McClure and Z. Kiss, J. Chem. Phys., 39, 3251 (1963).

18. N. Edelstein, W. Easley, and R. McLaughlin, Adv. Chem. Ser., 71, 203 (1967).

19. R. L. Fellows, J. R. Peterson, J. P. Young, and R. G. Haire, "The Rare Earths in Modern Science and Technology," G. J. McCarthy and J. J. Rhyne, eds., Plenum Publishing Corp., New York, 1978, pp. 493.

20. J. R. Peterson, R. L. Fellows, J. P. Young, and R. G. Haire, Radiochem. Radioanal. Ltrs., 31, 277 (1977).

21. J. F. Wild, E. K. Hulet, R. W. Lougheed, W. N. Hayes, J. R. Peterson, R. L. Fellows, and J. P. Young, J. Inorg. Nucl. Chem., 40, 811 (1978).

22. W. T. Carnall and H. M. Crosswhite, "Optical Spectra and Electronic Structure of Actinide Ions in Compounds and in Solution," ANL-84-90, 1985.

23. L. Brewer, J. Opt. Soc. Am., 61, 1101 (1971).

24. E. Loh, Phys. Rev., 154, 270 (1967).

25. J. F. Wyart, V. Kaufman, and J. Sugar, Physica Scripta, 22, 389 (1980).

26. C. H. H. Van Deurzen, K. Rajnak, and J. G. Conway, J. Opt. Soc. Am., B1, 45 (1984).

27. M. Genet, "Solid State Physics and Actinide Spectroscopy with $ThBr_4$," Report IPNO-DRE 84.02 (1984).

28. P. Delamoye, K. Rajnak, M. Genet, and N. Edelstein, Phys. Rev., B28, 4923 (1983).

29. P. Delamoye, J. C. Krupa, J. G. Conway, and N. Edelstein, Phys. Rev., B28, 4913 (1983).

30. J. C. Krupa, S. Hubert, M. Foyentin, E. Gamp, and N. Edelstein, J. Chem. Phys., 78, 2175 (1983).

31. E. Gamp, N. Edelstein, C. Khan Malek, S. Hubert, and M. Genet, J. Chem. Phys., 79, 2023 (1983).

32. D. R. Johnson, R. A. Satten, C. L. Schreiber, and E. Y. Wong, J. Chem. Phys., 44, 3141 (1966).

33. R. A., Satten, C. L. Schreiber, and E. Y. Wong, J. Chem. Phys., 78, 79 (1983).

34. F. Auzel and O. L. Malta, J. Physique, 44, 201 (1983).

35. H. M. Crosswhite, H. Crosswhite, W. T. Carnall, A. P. Paszek, J. Chem. Phys., 72, 5103 (1980).

36. F. Auzel, S. Hubert, P. Delamoye, and M. Hussonnois, J. Luminesc., 26, 251 (1982).

37. C. K. Jørgensen, Mol. Phys., 2, 96 (1959).

38. D. D. Ensor, J. R. Peterson, R. G. Haire, and J. P. Young, J. Inorg. Nucl. Chem., 43, 1001 (1981).

39. K. Rajnak, E. Gamp, R. Shinomoto, and N. Edelstein, J. Chem. Phys., 80, 5942 (1984).

40. K. Rajnak, R. H. Banks, E. Gamp, and N. Edelstein, J. Chem. Phys., 80, 5951 (1984).

41. H. G. Hecht, L. P. Varga, W. B. Lewis, and A. M. Boring, J. Chem. Phys., 70, 101 (1979).

42. L. R. Morss, C. W. Williams, and W. T. Carnall, ACS Sympos. Series, 216, 199 (1983).

43. H. G. Hecht, J. G. Malm, J. Foropoulos, and W. T. Carnall, Absts. of Papers Presented, Am. Chem. Soc. National Mtg., April 28 – May 3, 1985.

44. K. Eichberger and F. Lux, Ber. Bunsenges. Phys. Chem., 84, 800 (1980).

45. A. F. Leung and Y.-M. Poon, Can. J. Phys., 55, 937 (1977).

46. H. G. Hecht, J. G. Malm, and W. T. Carnall, J. Less-Common Metals, in press.

47. H.-D. Amberger, W. Grape, and E. Stumpp, J. Less-Common Metals, 95, 181 (1983).

48. K. C. Kim and G. A. Laguna, Chem. Phys. Ltrs., 82, 292 (1981).

49. Y.-M. Poon and D. J. Newman, J. Chem. Phys., 77, 1077 (1982).

50. H. G. Hecht, J. G. Malm, J. Foropoulos, and W. T. Carnall, research in progress, 1985.

51. J. V. Beitz, C. W. Williams, and W. T. Carnall, J. Chem. Phys., 76, 2756 (1982).

52. J. E. Barefield, II., W. W. Rice, J. J. Tiee and R. T. Walters, J. Chem. Phys., 79, 2621 (1983).

53. R. G. Denning, J. O. W. Norris, and P. J. Laing, Mol. Phys., 54, 713 (1985).

54. R. G. Denning, T. R. Snellgrove, and D. R. Woodwark, Mol. Phys., 32, 419 (1976).

55. R. G. Denning, T. R. Snellgrove, and D. R. Woodwark, Mol. Phys., 37, 1109 (1979).

56. C. K. Jørgensen and R. Reisfeld, Struct. Bonding, 50, 136 (1982).

57. R. L. DeKock, E. J. Baerends, P. M. Boerrigter, and J. G. Snijders, Chem. Phys. Ltrs., 105, 308 (1984).

58. R. G. Denning, J. O. W. Norris, and D. Brown, <u>Mol. Phys.</u>, <u>46</u>, 287 (1982).

59. R. G. Denning, J. O. W. Norris, and D. Brown, <u>Mol. Phys.</u>, <u>46</u>, 325 (1982).

60. N. G. Gorshkov and L. G. Mashirov, <u>Radiokhimiya</u>, <u>26</u>, 540 (1984).

Figure Captions

Figure 1.   Oxidation states of the actinides in which $5f^N \rightarrow 5f^N$ transitions have been observed.

Figure 2.   The effective operator model interactions for f^N-configurations.

Figure 3.   The solution absorption spectra of the trivalent actinides, U^{3+} through Es^{3+}, in dilute $HClO_4$ in the range 0-50000 cm^{-1}.

Figure 4.   A table of transition metals showing the crossover from elements with more d-like (itinerant) electron behavior to those with more f-like (localized) behavior.

Figure 5.   Variation of the Slater integral F^2 with atomic number: TOP, values computed using a Hartree-Fock code with a relativistic correction [HF(R)]; MID, values obtained by fitting experimental results (Expt); BOTTOM, the difference HF(R)-Expt.

Figure 6.   Spectra of $CfCl_2$ and $EsCl_2$ in the range 9000 - 20000 cm^{-1} based on results given in References 20 and 19, respectively.

Figure 7.   Estimated energies at which f→f transitions in An^{2+} ions may be observed and at which the lowest energy f→f transition will occur in the free-ion.

Figure 8.   The computed energy level structure for U(IV) as the free-ion, in the $ThBr_4$, Cs_2UCl_6, and $Hf(BD_4)_4$, together with the observed centers of gravity of absorption bands for U^{4+}(aquo).

Figure 9.   Energy levels of selected f^1-configurations.

Oxidation States of the Actinides in Which $5f^N \rightarrow 5f^N$ Transitions Have Been Characterized*

	Ac	Th	Pa	U	Np	Pu	Am	Cm	Bk	Cf	Es	Fm	Md	No	Lr
1+															
2+							■			■	■				
3+				○	○	○	○	○	○	○	○				
4+			△	△	△	△	△	△	△	△					
5+				■	■	■	■								
6+					■	■	■								
7+					■?										

*$5f^0$ cases such as Ac(III), Th(IV), ――― are omitted.

Effective Operator Model for f^N-Configuration

$$H = H_E + H_{SO} + H_{corr} + H_{CF}$$

$$H_E \text{ (electrostatic term)} = \sum_{k=0}^{6} F^k(nf,nf)f_k \qquad (k \text{ even})$$

$$H_{SO} \text{ (spin-orbit interaction)} = \zeta_{nf} \sum_{\text{electrons}} (s \cdot \ell)$$

H_{corr} = additional 2- and 3-body effective operators operating within the f^N-configuration -- partial correction for configuration interaction

$$H_{CF} \text{ (crystal-field interaction)} = \sum_{k,q,i} B_q^k (C_q^k)_i$$

Cm^{3+}

Bk^{3+}

Cf^{3+}

Es^{3+}

U^{3+}

Np^{3+}

Pu^{3+}

Am^{3+}

MOLAR ABSORPTIVITY

MOLAR ABSORPTIVITY

cm^{-1}

cm^{-1}

40

250

250

250

40

40

40

2500

2500

2500

2500

120

120

120

120

0

0

0

0

0 4000 8000 12000 16000 20000 24000 28000 32000 36000 40000 44000 48000

0 4000 8000 12000 16000 20000 24000 28000 32000 36000 40000 44000 48000

4f	La	Ce	Pr	Nd	Pm	Sm	Eu	Gd	Tb	Dy	Ho	Er	Tm
5f	Ac	Th	Pa	U	Np	Pu	Am	Cm	Bk	Cf	Es	Fm	Md
3d	Ca	Sc	Ti	V	Cr	Mn	Fe	Co	Ni	Cu			

Magnetic Moments

Bonding

[*d*-like (itinerant) → *f*-like (localized)]
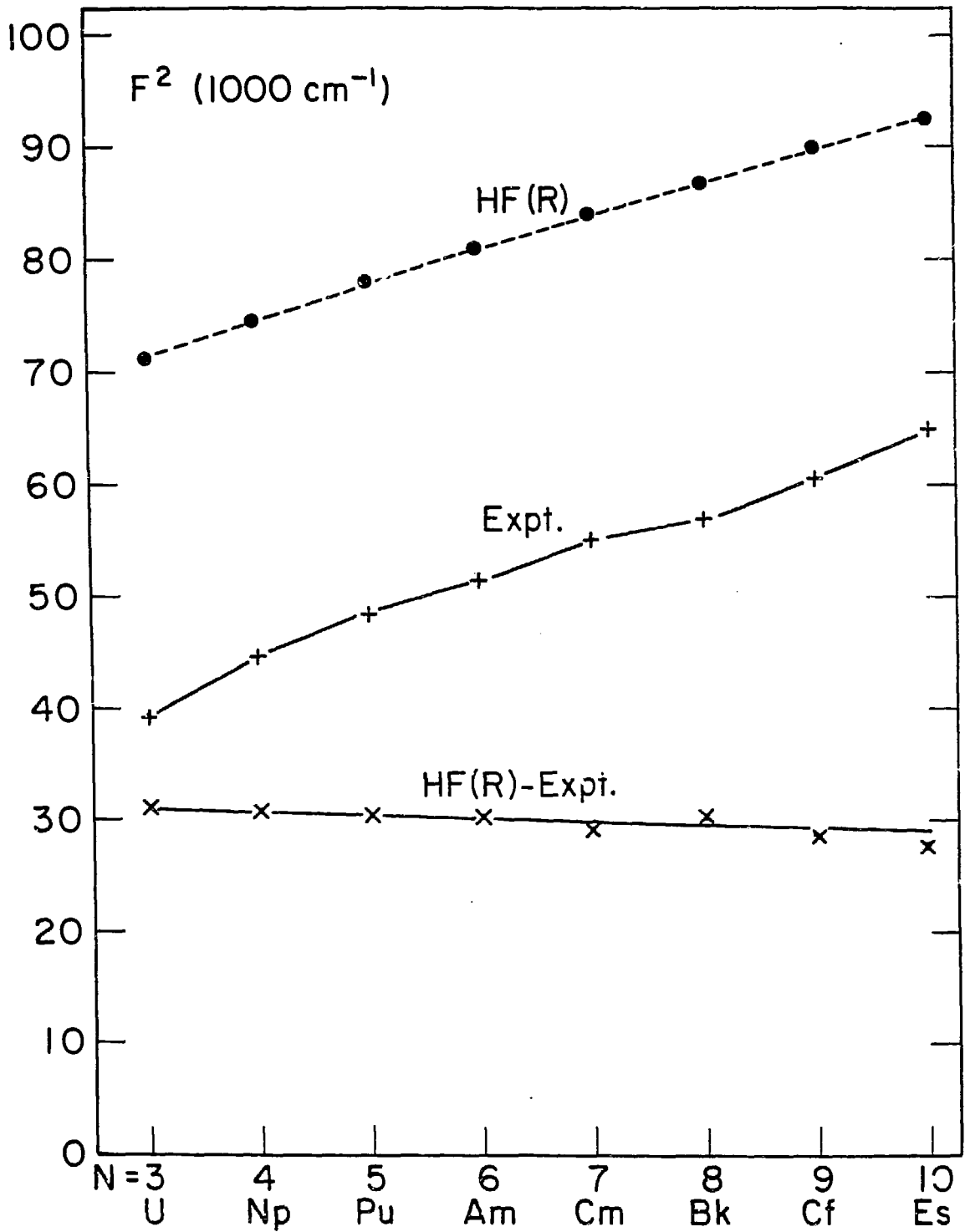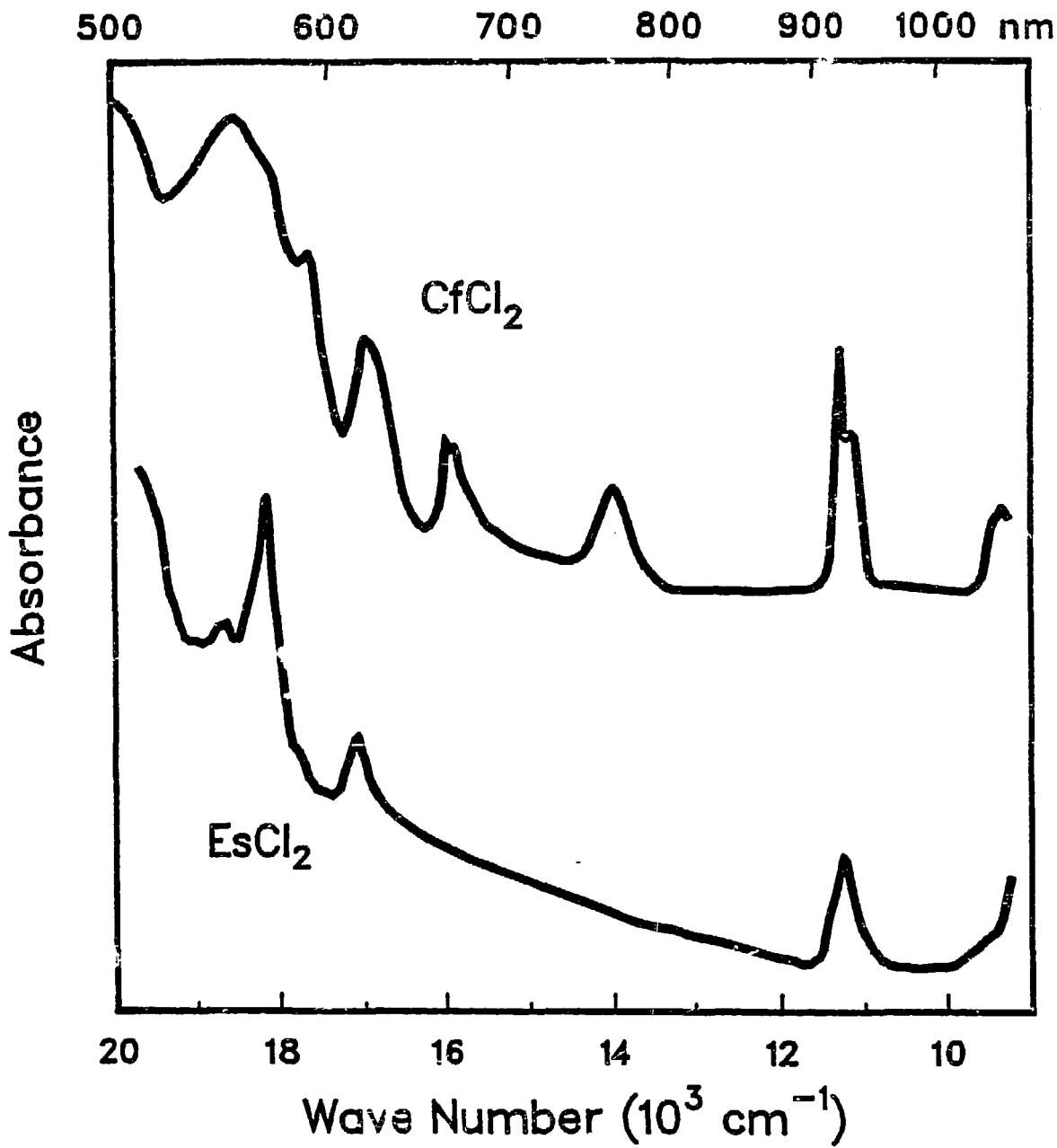
ESTIMATED RANGES OF ENERGY IN WHICH f→f TRANSITIONS IN An^{2+} IONS MAY BE OBSERVED

$cm^{-1} \times 10^3$

$^1S_0$ 93%

$^1S_0$

$^1S_0$

$^1S_0$

$^1S_0$

40 —

35 —

30 —

25 —

$^3P_2$ 66%

$^1D_2$

$^1D_2$

$^1I_6$ 95%

50% $^3P_2$

$^3P_2$

$^3P_2$

$^1G_4$

$^3P_1$ 100%

$^1I_6$

91%

$^1I_6$

$^1I_6$

$^1I_6$

20 —

90% $^3P_1$

$^3P_1$

$^3F_4$ 93%

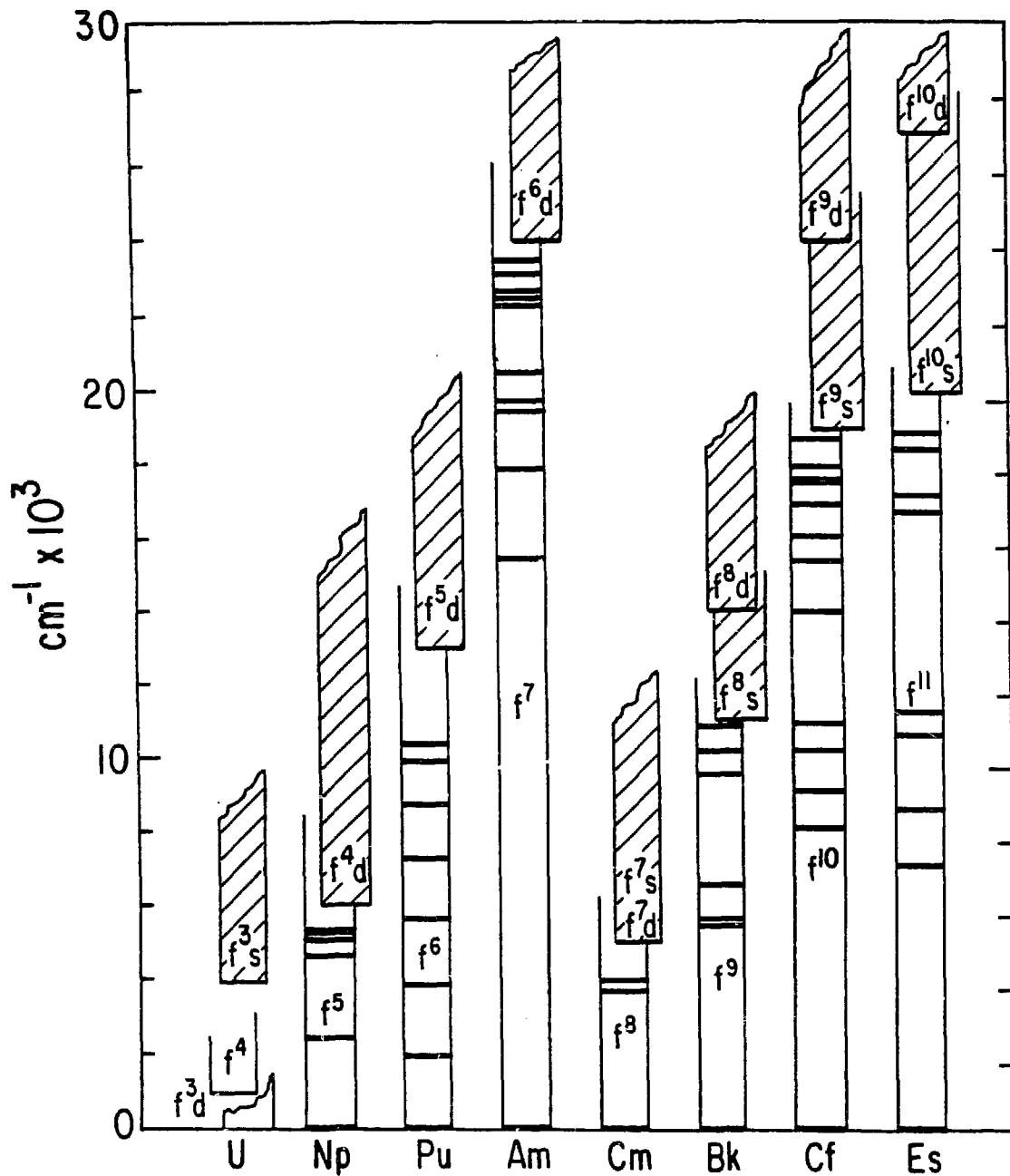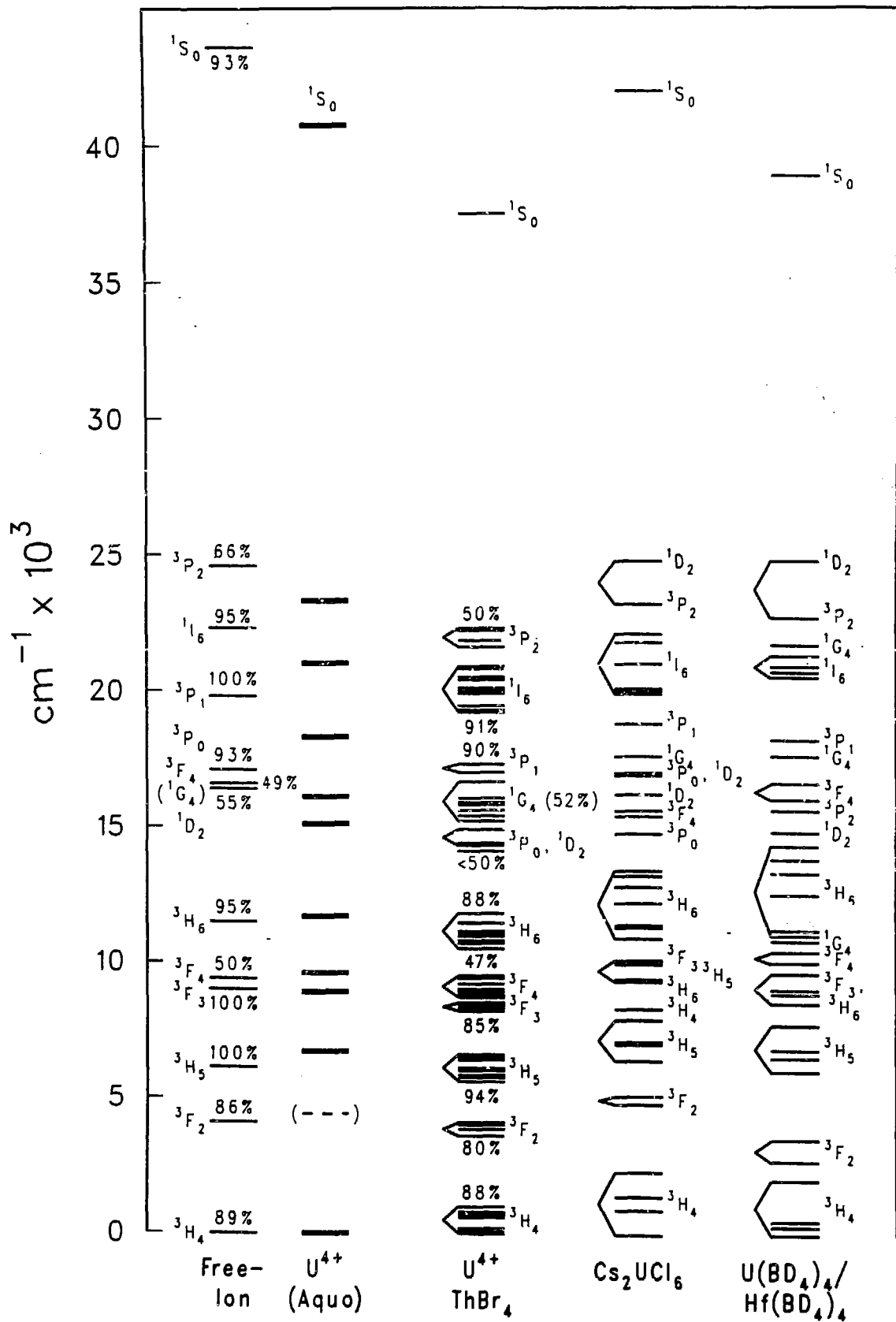$^1G_4 (52\%)$

$^1G_4$, $^3P_0$, $^1D_2$

$^3P_1$

$^3P_0$ 93%

$^1D_2$

$^1G_1$

($^1G_4$) 55% 49%

$^3F_4$

$^3F_4$

$^3P_0$, $^1D_2$

$^3P_2$

$^1D_2$

$^3P_0$

$^1D_2$

15 —

<50%

$^3H_6$

$^3H_6$ 95%

88% $^3H_6$

$^3H_6$

$^1G_4$

10 —

$^3F_4$ 50%

47%

$^3F_4$

$^3F_3$ $^3H_5$

$^3F_4$

$^3F_3$ 100%

$^3F_3$

$^3H_6$

$^3F_3$

85%

$^3H_4$

$^3H_6$

$^3H_5$ 100%

$^3H_5$

$^3H_5$

$^3H_5$

5 —

94%

$^3F_2$ 86%

(- - -)

$^3F_2$

$^3F_2$

80%

$^3F_2$

88%

0 —

$^3H_4$ 89%

$^3H_4$

$^3H_4$

$^3H_4$

Free-Ion | U^{4+} (Aquo) | U^{4+} ThBr$_4$ | Cs$_2$UCl$_6$ | U(BD$_4$)$_4$/Hf(BD$_4$)$_4$

Energy Levels of f^1-Configurations

$cm^{-1} \times 10^3$

Ce^{3+}
$Cs_2NaCeCl_6$

Pa^{4+}
Pa^{4+}: Cs_2ZrCl_6

U^{5+}
$LiUF_6$

Np^{6+}
NpF_6